ORIGINAL PAPER

Timothy M. LaPara · Alina C. Cole
John W. Shanahan · Michael J. Semmens

The effects of organic carbon, ammoniacal-nitrogen, and oxygen partial pressure on the stratification of membrane-aerated biofilms

Abstract The purpose of this study was to examine the effects of different nutrient (carbon, nitrogen, oxygen) concentrations on the microbial activity and community structure in membrane-aerated biofilms (MABs). MABs were grown under well-defined conditions of fluid flow, substrate concentration, and membrane oxygen partial pressure. Biofilms were then removed and thin-sliced using a cryostat/microtome parallel to the membrane. Individual slices were analyzed for changes with depth in biomass density, respiratory activity, and the population densities of ammonia-oxidizing and denitrifying bacteria populations. Oxygen-sensing microelectrodes were used to determine the depth of oxygen penetration into each biofilm. Our results demonstrated that ammonia-oxidizing bacteria grow near the membrane, while denitrifying bacteria grow a substantial distance from the membrane. However, nitrifying and denitrifying bacteria did not grow simultaneously when organic concentrations became too high or ammonia concentrations became too low. In conclusion, membrane-aerated biofilms exhibit substantial stratification with respect to community structure and activity. A fundamental understanding of the factors that control this stratification will help optimize the performance of full-scale membrane-aerated biofilm reactors for wastewater treatment.

Keywords Biofilms · Hybrid bioreactor · MABR · Membrane aeration · Nutrient removal

Introduction

All municipal and many industrial wastewaters contain carbonaceous and nitrogenous pollutants that would

T. M. LaPara (✉) · A. C. Cole · J. W. Shanahan · M. J. Semmens
Department of Civil Engineering, University of Minnesota,
122 Civil Engineering, 500 Pillsbury Drive SE,
Minneapolis, MN 55455, USA
E-mail: lapar001@umn.edu
Tel.: +1-612-6246028
Fax: +1-612-6267750

adversely affect surface water quality if they were released untreated. Numerous bioprocesses, therefore, have been developed to efficiently remove these pollutants from wastewaters. An emerging bioprocess technology is the membrane-aerated biofilm reactor (MABR), in which hydrophobic, gas-permeable membranes are used for bubbleless oxygen transfer [3, 4]. Membrane aeration is advantageous because gas transfer efficiencies are much higher than conventional bubble diffusers [3, 15], resulting in lower operating costs [3, 6, 15] and in reduced emission of volatile pollutants [3, 4].

Perhaps the most important feature of an MABR is its biofilm, which grows on the membrane surface and is responsible for metabolizing nutrients found in the wastewater. Membrane-aerated biofilms (MABs) have a fundamentally different stratification compared to biofilms grown on inert surfaces; oxygen and nutrients are provided from opposite sides of the biofilm, leading to a thicker zone of bacterial activity [8]. This unique biofilm stratification is particularly fortuitous in that the region near the membrane theoretically favors nitrification (i.e., rich in oxygen but poor in biodegradable organic compounds). Simultaneously, the region of the biofilm furthest from the membrane should favor denitrification (i.e., rich in biodegradable organic compounds plus the nitrate produced via nitrification, but poor in oxygen). Indeed, numerous studies have reported the concomitant removal of both carbonaceous and nitrogenous pollutants in a single-stage MABR [11, 12, 19, 23].

In conventional bioreactor designs for nitrification-denitrification, conditions are manipulated either in separate bioreactors (e.g., modified Ludzack Ettinger processes) [2] or temporally (e.g., sequencing batch reactors) [1] to enhance nitrification and denitrification rates. In MABRs, however, these biochemical processes occur within a single biofilm, such that the traditional manipulations are no longer applicable. Because MABRs achieve simultaneous nitrification–denitrification in a different manner than previous reactors designs, there is a substantial need to optimize MABR performance with respect to complete nitrogenous pollutant removal.

The objective of this study was to observe the effect of pertinent reactor conditions on the stratification of MABs. Our hypothesis is that nitrification–denitrification in MABRs is controlled by the mass transfer of nutrients into the biofilm, the relative concentrations of carbonaceous and nitrogenous compounds in the wastewater, and the relative quantity of oxygen transferred into the biofilm. We believed that relatively low concentrations of organic carbon would be beneficial for nitrifying bacteria but limit denitrification efficiency because of an insufficient quantity of electron donor. In contrast, excessive concentrations of organic carbon would inhibit the growth of nitrifying bacteria, which are outcompeted by heterotrophic populations when oxygen becomes limiting [16]. This inhibition of nitrification caused by excessive quantities of organic material, therefore, could be partially compensated by the provision of additional oxygen to the biofilm. To test these hypotheses, MABs were grown in laboratory flow-cell reactors, where variations in the stratification of these biofilms could be characterized under different fluid velocities, chemical oxygen demand (COD) concentrations, carbon:nitrogen (C:N) ratios, and intra-membrane oxygen partial pressures.

Materials and methods

Biofilm reactor

MABs were grown under three different well-defined conditions of fluid flow and substrate concentrations in a rectangular, closed flow-cell reactor (6 cm wide, 2.5 cm high, 2 m long) as previously described in detail [5]. Briefly, two biofilms were simultaneously grown on flat-sheet microporous membranes (20×1 cm) set into the base of the reactor, flush with the bottom of the tank. The reactor was inoculated with cryopreserved activated sludge (Metropolitan Wastewater Treatment Facility, St. Paul, MN). The hydraulic residence time in the growth chamber was kept short (6 h) to minimize the removal of nutrients such that biofilms could be grown at specifically targeted concentrations of COD and ammonia–nitrogen. Fluid velocities across the biofilms were controlled by the internal recirculation of reactor fluid using a centrifugal pump.

The reactor feed contained sodium acetate and ammonium chloride as the primary organic and nitrogenous components, respectively, in dechlorinated tap water; additional growth factors were provided by adding small quantities of yeast extract and casamino acids (2.5 mg l^{-1} each). Acetate was used as a carbon source because its diffusion rate is well-described, allowing our experimental results to be more easily compared to our model predictions [21]. In each biofilm growth experiment, the two membranes were supplied with 30 ml min^{-1} of either atmospheric air ($pO_2 = 0.21$ atm) or enriched oxygen ($pO_2 = 0.75$ atm),

both at atmospheric pressure. Actual reactor conditions are shown in Table 1.

Biofilms were removed from the reactor 8 to 10 weeks after inoculation. Samples ($\sim$1 cm×1 cm) were excised with a razor blade and immediately frozen at -15°C. The precise dimensions of each biofilm sample were determined with a vernier caliper. Biofilms were then thin-sliced at -15°C (typical thickness: 100–300 μm) parallel to the membrane in a combined cryostat/microtome (Richard-Allan Scientific, Kalamazoo, MI). Biofilm slices were transferred to sterile microcentrifuge tubes and stored separately at -20°C until further analysis.

Analytical methods

Reactor conditions were monitored three times each week. COD and nitrate–nitrogen concentrations were determined colorimetrically using the dichromate and NitraVer5 methods, respectively (Hach Co.; Loveland, CO). Ammonia–nitrogen was quantified using an ammonia-specific electrode (Hach).

Dissolved oxygen (DO) profiles were obtained from the biofilms using a Clark-type microelectrode (tip diameter = 10–15 μm; response time < 5 s; spatial resolution = 20–30 μm; Unisense, Denmark). The microelectrode was lowered through an access window in the top of the reactor and into the biofilm by a computer-controlled micromanipulator (Oriel Inst., Stratford, CT) capable of maneuvering in 0.1 μm increments. Biofilm thickness was determined using a 250× magnification microscope (Integrated Endoscopy; Irvine, CA) attached to a manually operated micromanipulator. DO profiles and thickness measurements were collected weekly in three locations centered on the middle of each biofilm. Biofilms were grown until DO profiles and thickness measurements suggested that growth had stabilized.

Respiratory activity was measured by iodonitrotetrazolium chloride (INT) reduction to INT-formazan [24]. Biofilm samples soaked in INT solution were incubated in the dark for 2 h at 40°C. After slicing, INT-formazan was extracted with 50% N,N-dimethylformamide in ethanol and incubated in the dark for 1 h. INT-formazan concentrations were quantified using a UV-Vis spectrophotometer ($\lambda = 464$ nm) (Beckman DU-530, Fullerton, CA). Killed-biofilm controls were soaked in 4% formaldehyde for 15 min.; these biofilms exhibited an activity of no more than 0.2 mmol e$^-$ l^{-1} h^{-1}.

Total particulate protein concentrations were quantified using the Lowry method [13]. Biofilm slices first were dried in a centrifugal drier (Labnet, Edison, NJ) and resuspended in 1.0 N NaOH. Protein was solubilized by incubation at 100°C for 10 min prior to analysis. The dry cell mass of large biofilm samples was quantified by incubating a known volume of biofilm at 103°C and weighing the residue with an analytical balance.

Table 1 The mean concentrations of nutrients under which membrane-aerated biofilms were grown

	COD	NH_3	O_2 concentration at the membrane
Condition 1			
Air-fed	100	26.5	9.1
O_2-fed	100	26.5	32.9
Condition 2			
Air-fed	97	9.9	8.9
O_2-fed	97	9.9	37.4
Condition 3			
Air-fed	198	21.4	7.8
O_2-fed	198	21.4	37.1

All concentrations are mg l^{-1}

Quantification of bacterial populations

For genomic DNA extraction, biofilm slices (slice volume: 10–30 µl) were suspended in 1 ml of lysis buffer [120 mM sodium phosphate buffer (pH 8.0), 5% sodium dodecyl sulfate], subjected to three successive freeze-thaw cycles, and incubated at 70°C for 90 min. Genomic DNA was extracted and purified from these samples using the FastDNA Spin Kit per manufacturer's instructions (QBioGene; Vista, CA).

Nitrosomonas oligotropha-like populations were quantified in each biofilm slice by competitive PCR (cPCR) of ammonia monoxygenase (*amoA*) gene fragments using primers AMO598F and AMO718R [7]. A competitor [7] of 100 nucleotides in length was synthesized by AlphaDNA (Montreal, Canada). PCR reaction mixtures (50 µl) contained: 1× PCR buffer (Promega; Madison, WI), 175 µmol $MgCl_2$, 4 nmol deoxynucleoside triphosphates, 2% bovine serum albumin, 25 pmol forward and reverse primers, 1.25 units of Ampli*Taq* polymerase (Roche Diagnostics; Indianapolis, Ind.) and ~1 ng of total genomic DNA. The PCR protocol included a 5 min initial denaturation at 94°C, forty cycles of 94°C for 1 min, 60°C for 1 min, and 72°C for 1 min, and a final extension for 7 min at 72°C.

For each biofilm sample slice (target), competitive PCR amplifications were performed on four mixtures containing a constant target DNA concentration and decreasing competitor copy numbers. Products were resolved on a 3% w/v NuSieve 3:1 agarose gel (Bio-Whittaker, Rockland, Maine) in 1× Tris-borate-EDTA (TBE) buffer [17] stained with ethidium bromide. Band intensities of target DNA and competitor DNA were quantified using LabWorks Image Acquisition software (UVP).

Denitrifying bacterial populations were quantified by cPCR of two functionally redundant nitrite reductase gene fragments (*nirS* and *nirK*). Competitors for these cPCR reactions were synthesized as described previously [5]. The PCR reaction mixtures for cPCR of *nirS* and *nirK* gene fragments were the same as described above except that different primer pairs were used (*nirS*: cd3 F and cd4 R; *nirK*: F1aCu and R3Cu) [10, 14]. The PCR protocol for the amplification of *nirS* gene fragments included a 5 min initial denaturation at 94°C, 40 cycles of 94°C for 1 min, 50°C for 1 min, and 72°C for 1.5 min, and a final extension for 10 min at 72°C. The PCR protocol for the amplification of *nirK* gene fragments included a 3 min initial denaturation at 94°C, 35 cycles of 94°C for 0.5 min, 57°C for 1 min, and 72°C for 1 min, and a final extension for 10 min at 72°C. cPCR products were resolved on 2% agarose gels (Bio-Rad; Hercules, Calif.) in 1× Tris-acetate-EDTA (TAE) buffer [17] and stained with ethidium bromide.

Data analysis

INT-F concentrations (mg ml^{-1}) measured in the biofilms were converted to an equivalent respiration rate (mmol e^- l^{-1} h^{-1}) by multiplying by the number of electron equivalents required for formazan production (2 mol e^- per mol formazan) and dividing by the contact time (2 h) [22]. Total respiratory activity was estimated as the area under the curve of the plot of INT-formazan-based respiratory activity versus distance from membrane by the trapezoidal rule.

For all competitive PCR assays, the target copy number was determined as the value of the *y*-intercept of a linear regression of the log of the competitor copy number versus the log of the ratio of target to corrected competitor band intensity. Competitor band intensity was corrected for the difference in amplicon length between the actual target and competitor by multiplication by a factor of 121/100, 735/633 and 474/415 for *amoA*, *nirS* and *nirK*, respectively. Total quantities of ammonia-oxidizing bacteria (AOB) and denitrifying bacteria were computed as the area under the curve of the plot of gene copy number versus distance from membrane by the trapezoidal rule.

Results

Biofilm thickness and biomass density

Biofilms rapidly grew over the first 3 weeks of each experiment (data not shown), but then biofilm thicknesses generally stabilized with respect to time during the last few weeks of each experiment (Fig. 1). The thickness of one of the biofilms (oxygen-fed, Condition 1), however, continued to increase in thickness throughout the experiment. In general, the oxygen-fed biofilms were thicker than the air-fed biofilms grown under the same conditions. Similarly, nutrient concentrations substantially impacted biofilm thickness. Making pairwise comparisons, a 2.5-fold increase in NH_3 concentration (i.e., Condition 2 vs. Condition 1) resulted in a 1.4-fold increase in biofilm thickness (air-fed biofilms only); a 2-fold increase in COD concentration resulted in a 20–50% increase in biomass thickness (i.e., Condition 2 vs. Condition 3) (Table 2).
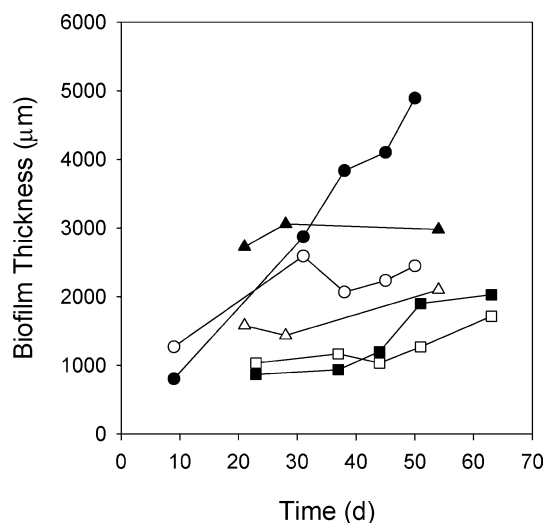
Fig. 1 The thickness of membrane-aerated biofilms grown under three different chemical conditions (Table 1). *Filled circle*, Condition 1, air-fed; *open circle*, Condition 1, oxygen-fed; *filled square*, Condition 2, air-fed; *open square*, Condition 2, oxygen-fed; *filled triangle*, Condition 3, air-fed; *open triangle*, Condition 3, oxygen-fed

Biomass densities (measured as total protein) also varied substantially as a function of depth within some of the biofilms as well as a function of reactor conditions (Fig. 2). The biomass densities were similar for the air-fed and oxygen-fed biofilms under all three conditions. Under Conditions 1 and 2, the highest biomass densities were observed near the membrane; biomass densities declined as function of distance from the membrane. Under Condition 3, the biomass density was relatively constant as a function of distance from the membrane. The ratio of cellular protein to dry cell mass in these biofilms was 3–16%.

Dissolved oxygen penetration and respiratory activity

Oxygen penetration into the biofilms varied substantially between experimental conditions (Fig. 3). The oxygen-fed biofilms exhibited substantially deeper oxygen penetration as well as higher oxygen fluxes (Table 2) into the biofilm than the air-fed biofilms. All of the oxygen profiles were initially linear as a function of distance from the membrane, suggesting that mass transfer was controlled by diffusion rather than bacterial uptake. In the biofilms grown under Condition 2, the oxygen concentration profiles remained largely linear until oxygen was no longer detectable. In contrast, the oxygen concentration profiles in the biofilms grown under Conditions 1 and 3 flattened as the oxygen concentrations neared zero, suggesting that bacterial respiration had a minimal effect on the oxygen flux across the membrane.

The differences in experimental conditions produced substantially different respiratory activity profiles in the MABs (Fig. 4). The biofilms grown under Conditions 1 and 2 exhibited hump-shaped respiratory profiles as a function of distance from the membrane. In contrast, the biofilms grown under Condition 3 exhibited relatively constant respiratory activity as a function of distance from the membrane. The profiles of respiratory activity were generally consistent with the dissolved oxygen profiles. For the biofilms grown under Conditions 1 and 2, the location of the highest bacterial respiratory activity roughly corresponded to the location at which dissolved oxygen was depleted; this is reasonable for biofilms with anti-parallel provision of electron donor (i.e., from the bulk fluid) and electron acceptor (i.e., through the membrane). In contrast, the dissolved oxygen and respiratory activity profiles for the biofilms grown under Condition 3 suggested that there was substantial bacterial activity throughout the depth of the biofilm.

Profiles of ammonia-oxidizing and denitrifying bacteria

Ammonia-oxidizing bacteria (AOB) and denitrifying bacteria were simultaneously detected in only one of the air-fed biofilms (Fig. 5). Under Condition 1, AOB were detected near the membrane, and their concentration declined as the distance from the membrane increased (Fig. 5a). Two different profiles were observed for the *nirK*- and *nirS*-type denitrifying bacteria under Condition 1. The *nirK*-type denitrifying bacteria were detected throughout the biofilm, although their highest concentration occurred in the middle of the biofilm. The *nirS*-type denitrifying bacteria were not detectable near the

Table 2 Summary of the characteristics of the membrane-aerated biofilms analyzed in this study

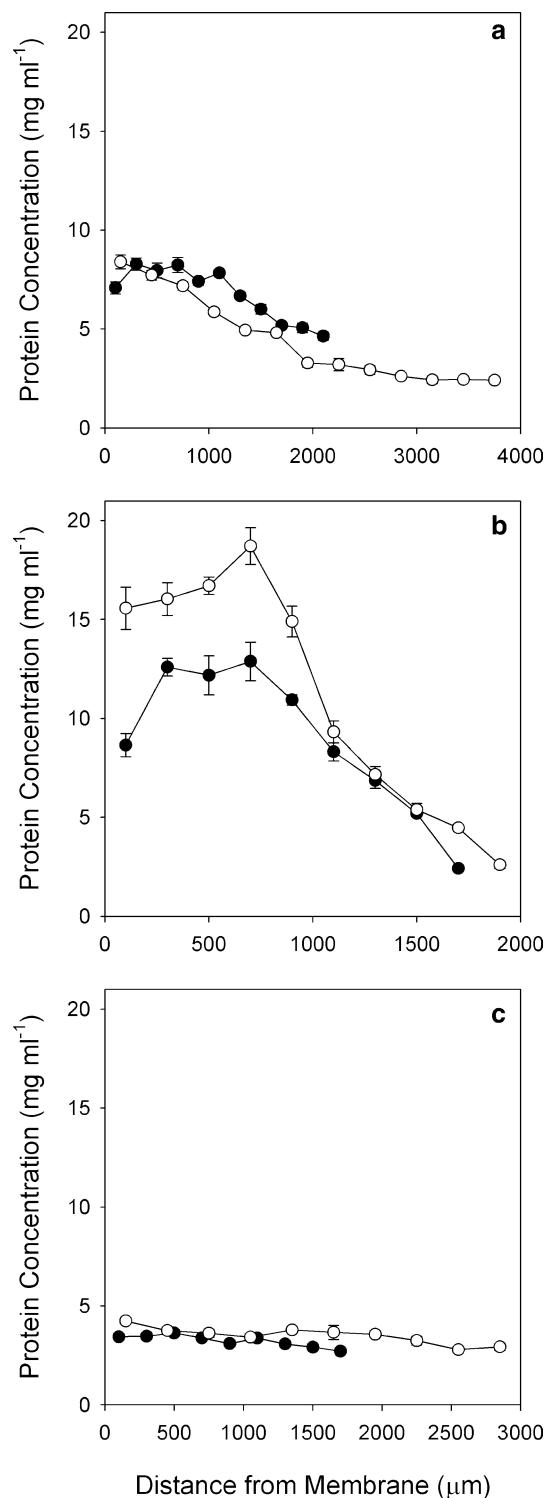|	Final thickness (mm)	Mean protein biomass (mg ml^{-1})	Dry cell mass (mg ml^{-1})	O$_2$ flux (mg min^{-1} m^{-2})	Total respiratory activity (mmol e m^{-2} h^{-1})	Total *amoA* (copies mm^{-2})	Total *NirK* (copies mm^{-2})	Total *nirS* (copies mm^{-2})
Condition 1								
Air-fed	2.4	6.8	70	2.2	6.9	2,540	4,600	8,900
O$_2$-fed	4.9	4.5	66	3.9	14.1	2,900	1,840	4,870
Condition 2								
Air-fed	1.7	8.9	81	4.0	4.7	0	60	4,100
O$_2$-fed	2.0	11.1	81	5.8	7.8	5,100	5,100	5,000
Condition 3								
Air-fed	2.1	1.8	52	1.5	3.5	0	100	225
O$_2$-fed	3.0	2.7	17	2.3	5.4	0	25	70

Fig. 2 Protein concentration profiles of air-fed (*closed symbols*) and oxygen-fed (*open symbols*) membrane-aerated biofilms grown under three different conditions. **a** Condition 1; **b** Condition 2; **c** Condition 3

membrane, but then became quite prominent near the liquid–biofilm interface.

AOB were not detected in either of the air-fed biofilms grown under Conditions 2 and 3 (Fig. 5b, c). Both

nirK- and nirS-type denitrifying bacteria were detected in the air-fed biofilm grown under Condition 2 (Fig. 5b), which was unexpected given that no nitrifying bacteria were detectable in this biofilm—although AOB were detected in the oxygen-fed biofilm grown concomitantly under this condition (Fig. 6b). Only small quantities of denitrifying bacteria were detected in the air-fed biofilm grown under Condition 3 (Fig. 5c).

The oxygen-fed biofilms grown under Conditions 1 and 3 produced similar profiles of ammonia oxidizing and denitrifying bacteria as the air-fed biofilms concomitantly grown under the same conditions (Fig. 6a, c). In contrast, the oxygen-fed biofilm grown under Condition 2 (Fig. 6b) had substantially different population profiles than the corresponding air-fed biofilm (Fig. 5b). In this oxygen-fed biofilm, AOB were detected throughout a substantial fraction ($\sim$75%) of the biofilm thickness. Both the nirK- and nirS-types of denitrifying bacteria were also detected throughout the biofilm.

Discussion

Our long-term research goal is to optimize simultaneous nitrification–denitrification in MABRs, which are unique in their ability to achieve complete nitrogenous pollutant removal by promoting the growth of nitrifying and denitrifying bacterial communities within a single biofilm (separated by a few millimeters or less). Consistently achieving the desired stratification of bacterial populations, however, poses a difficult bioengineering challenge. In many ways, the future design of MABRs will require a paradigm shift from current wastewater treatment engineering practices because these systems will need to be fabricated to specifically accommodate the ecological interaction of nitrifying and denitrifying bacterial populations. Previous researchers have termed this design paradigm as "ecological engineering" [9] or "sludge population optimization" [25]. In our recent research, we developed a mathematical model to predict the stratification of nitrifying and denitrifying bacterial populations [21]. These predictions were corroborated by a preliminary experimental study in which the proposed stratification of AOB and denitrifying bacteria was confirmed [5].

In the current study, we manipulated the concentrations of key nutrients (organic carbon, ammonia–nitrogen, and oxygen) to discern their effect on the growth and stratification of MABs. For MABs grown under relatively low concentrations of COD but high concentrations of ammonia (Condition 1), the AOB and denitrifying bacteria stratified as a function of depth in a manner that was consistent with our original hypothesis (Figs. 5a, 6a). When MABs were grown with a similar COD concentration but lower ammonia concentration (Condition 2), the AOB failed to grow in the air-fed biofilm (Fig. 5b), although additional oxygen transfer to the biofilm did promote the growth of both AOB and denitrifying

320

Fig. 3 Dissolved oxygen
profiles in membrane-aerated
biofilms grown under three
different conditions.
a Condition 1, air-fed;
b Condition 1, oxygen-fed;
c Condition 2, air-fed;
d Condition 2, oxygen-fed;
e Condition 3, air-fed;
f Condition 3, oxygen-fed
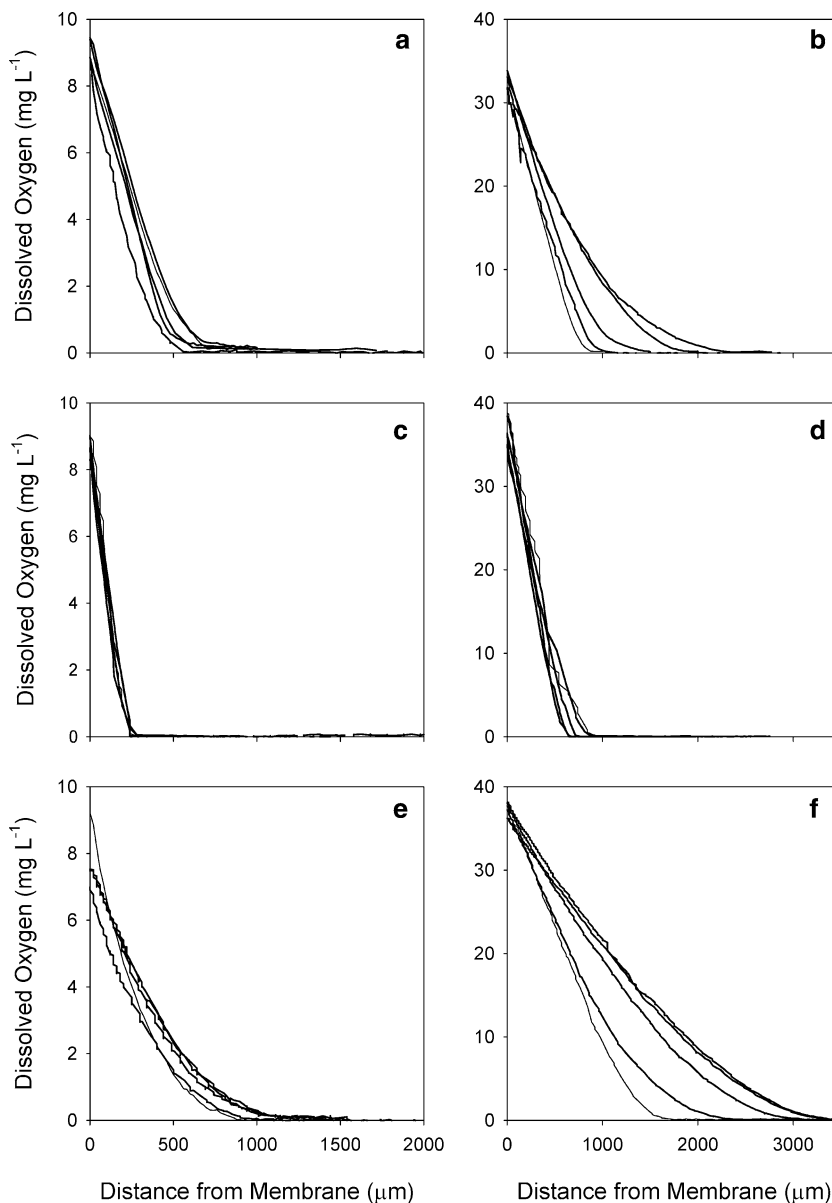
bacteria (Fig. 6b). In contrast, no AOB were detected
when MABs were grown under a high COD concentra-
tion and a low ammonia concentration regardless of how
much oxygen was fed to the biofilm (Figs. 5c, 6c).

These results confirm our original hypotheses with
respect to the conditions under which the stratification
of AOB and denitrifying bacteria will occur in MABs. If
the organic content becomes too high, then aerobic
heterotrophic bacteria will outcompete the AOB for
oxygen [16], preventing nitrification from proceeding.
We hypothesize that this inhibition can be relieved by
increasing membrane surface area to provide more
oxygen to the biofilms (or by using enriched oxygen).
Furthermore, the ratio of organic nutrients to ammo-
nia–nitrogen can be an important factor in the devel-
opment of this stratification. At high carbon to nitrogen
ratios, the heterotrophic bacteria can conceivably out-
compete the AOB for ammonia. In contrast, low carbon

to nitrogen ratios would allow nitrification to proceed,
but denitrification would be limited by the availability of
electron donor. Based on our modeling efforts [21],
experimental results and stoichiometric calculations, we
conclude that nitrification–denitrification will be opti-
mum at a COD:N ratio of 4:1 in MABRs.

Although our modeling efforts have identified key
parameters that control the development of MABs [8,
21], our experimental results reveal several limitations of
our mathematical model. In particular, the MABs were
often quite heterogenous with respect to biomass density
as a function of depth (Fig. 2a, b). This heterogeneity
would substantially affect model predictions for mass
transfer of nutrients within the biofilm and for the rates
of bacterial metabolism within the MABs [20].

In spite of these limitations, however, our experi-
mental results support our model prediction of bacterial
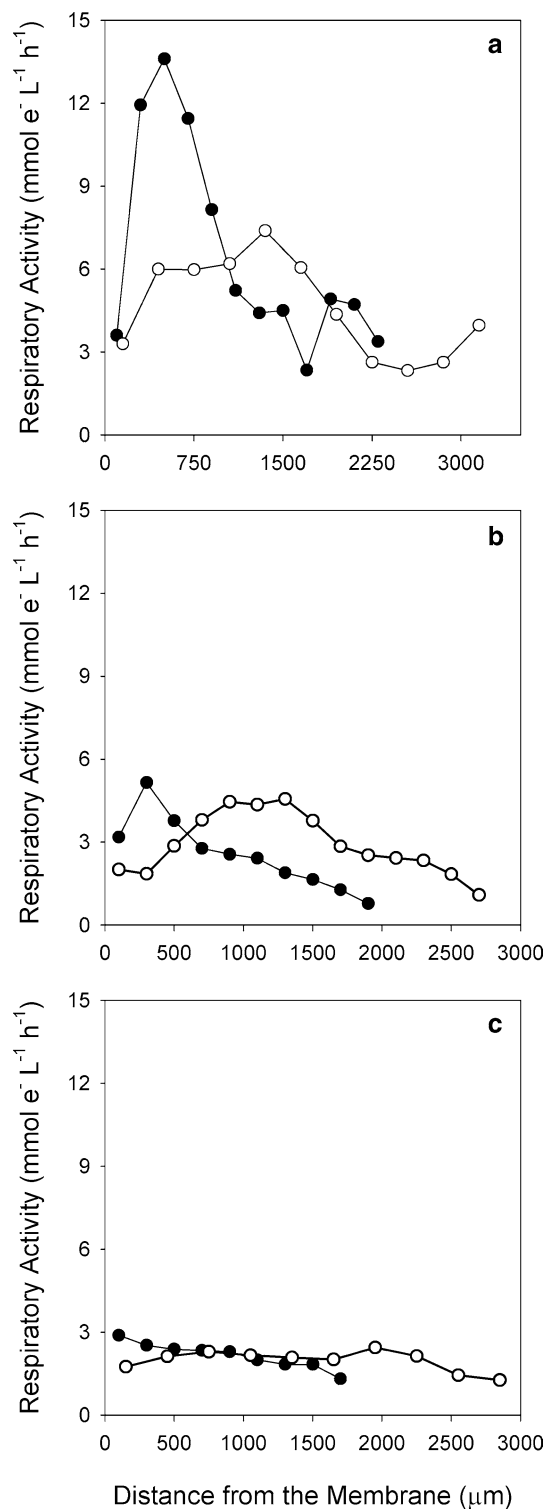activity as a function of depth, suggesting that our

Fig. 4 Profiles of respiratory activity as functions of depth in air-fed (*closed symbols*) and oxygen-fed (*open symbols*) membrane-aerated biofilms grown under different conditions. **a** Condition 1; **b** Condition 2; **c** Condition 3

Fig. 5 Population profiles of AOB and denitrifying bacteria in air-fed membrane-aerated biofilms as quantified by competitive quantitative PCR of *amoA* (*filled circle*), *nirS* (*open triangle*), and *nirK* (*open square*) gene fragments. **a** Condition 1; **b** Condition 2; **c** Condition 3

model offers a substantial opportunity to understand the ecology of MABs [8]. This hump-shaped profile of respiratory activity, however, has several consequences for MABR performance. The relatively low respiratory
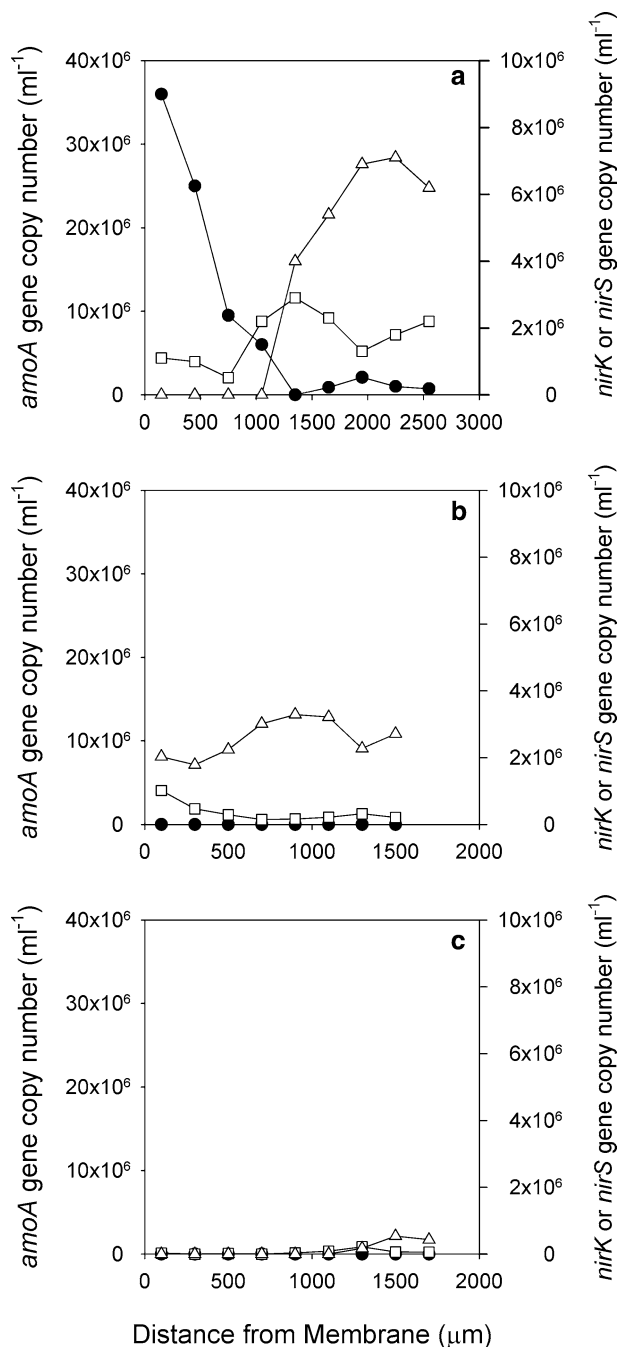
activity near the membrane effectively represents a diffusional barrier hindering oxygen transfer to the biofilm; this hypothesis is supported by our empirical observation of linear DO profiles as a function of depth near the membrane. Presumably, an analogous barrier also exists on the biofilm-liquid side that hinders the mass transfer of biodegradable organic compounds and ammonia into the biofilm. Biofilm thickness, therefore,
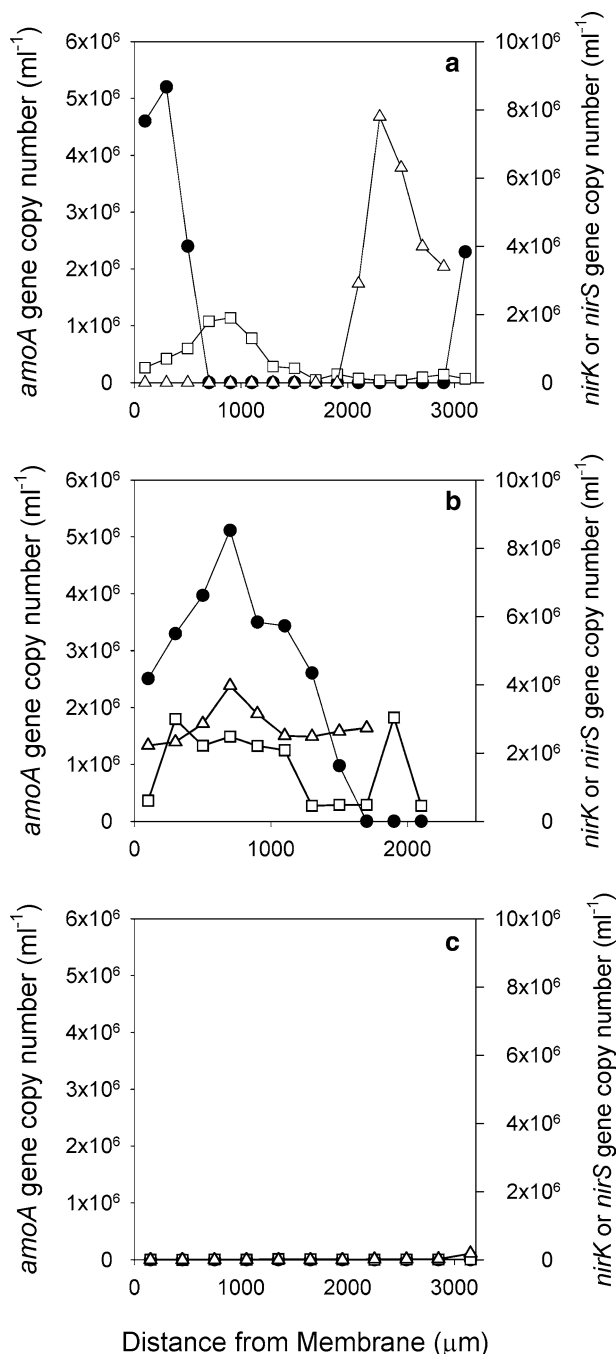
Fig. 6 Population profiles of AOB and denitrifying bacteria in oxygen-fed membrane-aerated biofilms as quantified by competitive quantitative PCR of *amoA* (*filled circle*), *nirS* (*open triangle*), and *nirK* (*open square*) gene fragments. **a** Condition 1; **b** Condition 2; **c** Condition 3

contrast, most wastewater treatment bioreactors are operated such that the in situ concentrations of COD and ammonia are low. Numerous previous studies, however, have demonstrated that AOB and denitrifying bacteria can grow under these conditions [11, 18, 23]. Our study is also limited by the destructive nature of biofilm removal and slicing, which limited our ability to perform replicate analyses of our biofilms.

In conclusion, our research demonstrates that AOB and denitrifying bacteria can simultaneously grow in MABs. The AOB grow near the membrane, which contains sufficient oxygen (Fig. 3), but is likely low in biodegradable organic carbon. The denitrifying bacteria grow a substantial distance from the membrane, where anoxic conditions persist and presumably there is a sufficient quantity of biodegradable organic carbon. The relative concentrations of biodegradable organic carbon and ammonia, however, can play an important role in the simultaneous development of AOB and denitrifying bacteria. To a limited extent, the desired stratification can be manipulated by increasing the quantity of oxygen transferred to MABs.

References

1. Alleman JE, Irvine RL (1980) Storage-induced denitrification using sequencing batch reactor operation. Water Res 14:1483–1488
2. Barnard JL (1975) Biological nutrient removal without the addition of chemicals. Water Res 9:485–490
3. Brindle K, Stephenson T (1996) The application of membrane biological reactors for the treatment of wastewaters. Biotechnol Bioengin 49:601–610
4. Casey E, Glennon B, Hamer G (1999) Review of membrane-aerated biofilm reactors. Resour Conserv Recyl 27:203–215
5. Cole AC, Semmens MJ, LaPara TM (2004) Stratification of activity and bacterial community structure in biofilms grown on membranes transferring oxygen. Appl Environ Microbiol 70:1982–1989
6. Côté P, Bersillon J-L, Huyard A, Faup G (1988) Bubble-free aeration using membranes: process analysis. J Wat Pollut Control Fed 60:1986–1992
7. Dionisi HM, Layton AC, Harms G, Gregory IR, Robinson KG, Sayler GS (2002) Quantification of *Nitrosomonas oligotropha*-like ammonia-oxidizing bacteria and *Nitrospira* spp. from full-scale wastewater treatment plants by competitive PCR. Appl Environ Microbiol:68:245–253
8. Essila NJ, Semmens MJ, Voller VR (2000) Modeling biofilms on gas-permeable supports: concentration and activity profiles. J Environ Eng 126:250–257
9. Grady CPL, Filipe CDM (2000) Ecological engineering for bioreactor for wastewater treatment. Wat Air Soil Pollut 123:117–132
10. Hallin S, Lindgren P-E (1999) PCR detection of genes encoding nitrite reductase in denitrifying bacteria. Appl Environ Microbiol 65:1652–1657
11. Hibiya K, Terada A, Tsuneda S, Hirata A (2003) Simultaneous nitrification and denitrification by controlling vertical and horizontal microenvironment in a membrane-aerated biofilm reactor. J Biotechnol 100:23–32

needs to be sufficiently thick to allow both nitrification and denitrification to proceed, but not excessively thick such that bacterial activity is adversely affected.

A limitation of the current study is the contrived conditions under which the MABs were grown. The experimental design involved small membrane areas and short hydraulic residence times such that the COD and ammonia concentrations could be easily controlled. In

12. Kappell AS, Semmens MJ, Novak PJ, LaPara TM (2005) Novel application of oxygen-transferring membranes to improve anaerobic wastewater treatment. Biotechnol Bioengin 89:373–380

13. Lowry OH, Rosebrough NJ, Farr AL, Randall RJ (1951) Protein measurement with the Folin phenol reagent. J Biol Chem 193:265–275

14. Michotey V, Méjean V, Bonin P (2000) Comparison of method for quantification of cytochrome cd_1-denitrifying bacteria in environmental marine samples. Appl Environ Microbiol 66:1564–1571

15. Pankhania T, Stephenson T, Semmens MJ (1994) Hollow fiber bioreactor for wastewater treatment using bubbleless membrane aeration. Wat Res 28:233–2236

16. Rittmann BE (1987) Aerobic biological treatment. Environ Sci Technol 21:128–136

17. Sambrook J, Fritsch EF, Maniatis T (1989) Molecular cloning: a laboratory manual, 2nd edn. Cold Spring Harbor Laboratory, Cold Spring

18. Satoh H, Ono H, Rulin B, Kamo J, Okabe S, Fukushi KI (2004) Macroscale and microscale analyses of nitrification and denitrification in biofilms attached on membrane-aerated biofilm reactors. Wat Res 38:1633–1641

19. Semmens MJ, Dahm K, Shanahan J, Christianson A (2003) COD and nitrogen removal by biofilms growing on gas permeable membranes. Wat Res 37:4343–4350

20. Shanahan JW, Cole AC, Semmens MJ, LaPara TM (2005) Acetate and ammonium diffusivity in membrane-aerated biofilms: improving model predictions using experimental results. Wat Sci Technol, in press

21. Shanahan JW, Semmens MJ (2004) Multi-population model of membrane-aerated biofilms. Environ Sci Technol 38:3176–3183

22. Smith JJ, McFeters GA (1997) Mechanisms of INT (2-(4-iodophenyl)-3-(4-nitrophenyl)-5-phenyl tetrazolium chloride), and CTC (5-cyano-2,3-ditolyl tetrazolium chloride) reduction in *Escherichia coli* K-12. J Microbiol Meth 29:161–175

23. Terada K, Hibiya K, Nagai J, Tsuneda S, Hirata A (2003) Nitrogen removal characteristics and biofilm analysis of a membrane-aerated biofilm reactor applicable to high-strength nitrogenous wastewater treatment. J Biosci Bioengin 95:170–178

24. von Mersi W, Schinner F (1991) An improved and accurate method for determining the dehydrogenase activity of soils with iodonitrotetrazolium chloride. Biol Fert Soils 11:216–220

25. Yuan Z, Blackall LL (2002) Sludge population optimization: a new dimension for the control of biological wastewater treatment systems. Wat Res 36:482–490